


Effects of Selenium Nanoparticles Using Potential Natural Compounds Naringenin and Baicalin for Diabetes

Rosa Martha Pérez Gutiérrez ^{1,*} , Julio Téllez Gómez ², Felipe Fernando Martínez Jerónimo ³, Silvia Patricia Paredes-Carrera ⁴, Jesús Carlos Sánchez-Ochoa ⁴

¹ Natural Products Research Laboratory. Higher School of Chemical Engineering and Extractive Industries. National Polytechnic Institute (IPN)/Laboratorio de Investigación de Productos Naturales. Escuela Superior de ingeniería Química e Industrias Extractivas. Instituto Politécnico Nacional (IPN) Unidad Profesional Adolfo López Mateos S/N Av. Instituto Politécnico Nacional Ciudad de México, cp 07708, México

² Anahuac Center for Research in Psychology, Faculty of Psychology Universidad Anahuac / Centro Anáhuac de Investigación en Psicología, Facultad de Psicología Universidad Anáhuac, Av. Universidad Anáhuac 46, Huixquilucan Edo. De Mex. México

³ National School of Biological Sciences, Experimental Hydrobiology Laboratory / Escuela Nacional de Ciencias Biológicas, Laboratorio de Hidrobiología Experimental, Carpio y Plan de Ayala S/N, Col. Santo Tomás, CDMX 11340, México

⁴ Sustainable Nanomaterials Laboratory. Postgraduate Studies and Research Section - Higher School of Chemical Engineering and Extractive Industries, National Polytechnic Institute / Laboratorio de Nanomateriales Sustentables. Sección de Estudios de Posgrado e Investigación - Escuela Superior de Ingeniería Química e Industrias Extractivas, Instituto Politécnico Nacional, Av. Instituto Politécnico Nacional S/N, Unidad Profesional Adolfo López Mateos, CP 07708 CDMX, México

* Correspondence: rmpg@prodigy.net.mx (R.M.P.G.);

Scopus Author ID 6602069565

Received: 4.01.2023; Accepted: 9.02.2023; Published: 11.04.2023

Abstract: Current investigation aimed to evaluate a formulation of selenium nanoparticles (SeNPs) using Naringenin/Baicalin in streptozotocin-induced diabetic mice and INS-1 pancreatic β -cells. Nanoparticles were characterized using Fourier Transform-infrared, ultra-violet-visible, scanning electron microscopy, energy-dispersive X-ray spectroscopy, and Zetasizer showing the existence of NAR/BAI on the surface of Se NPs. NAR/BAI/SeNPs have sizer ranging between 80 nm and 119 nm, showing a negative potential of -22.3 mV and a polydispersity index (PDI) of -0.249, indicating that they form a stable dispersion with stability within five months. The EE and LC flavonoids-loaded NPs were 80.1% and 25.4%, respectively. All parameter biochemical were altered by diabetic induction in mice; after 8 weeks of treatment, blood glucose, insulin levels, lipid profile, and glycosylated hemoglobin exhibited significant glucose and insulin effect in the oral glucose tolerance test, indicating improved insulin resistance. In the liver, NAR/BAI/SeNPs increase superoxide dismutase, Catalase glutathione peroxidase, as well as reduce lipid peroxidation, and transaminases aspartate aminotransferase, alanine aminotransferase, and alkaline phosphatase activities improved liver function elevating liver and muscle glycogen content, protects pancreatic b cells against high glucose-induced damage due to its synergistic effect between selenium with flavonoids. According to the results, NAR/BAI/SeNPs exhibit an anti-diabetic effect protecting and repairing pancreatic b cells.

Keywords: naringenin; baicalin; nanoparticles; selenium; diabetes; antioxidant

© 2023 by the authors. This article is an open-access article distributed under the terms and conditions of the Creative Commons Attribution (CC BY) license (<https://creativecommons.org/licenses/by/4.0/>).

1. Introduction

Diabetes mellitus is a metabolic disease characterized by insulin resistance and decreased insulin secretion; as a consequence, chronic hyperglycemia brings severe long-term

health complications. Diabetes is one of the main diseases of our society due to chronic hyperglycemia, which modifies a large number of organs producing serious secondary pathologies [1]. Although experimental studies and clinical evidence have shown that in the development of diabetes, one remarkable mechanism involved is oxidative stress and its attendant complications [2], several hypoglycemic drugs are commonly used to treat diabetes mellitus type 2 (T2DM), including acarbose insulin, metformin thiazolidinediones, and rosiglitazone. Nevertheless, these synthetic drugs result in drug resistance and acute side effects [3].

T2DM can be induced in rodents with streptozotocin due it generates reactive oxygen species (ROS), playing a crucial role in the cytotoxicity of STZ [4]; interferes in the β cell via glucose transporter (GLUT2), causing alkylation of DNA. Consequently, β cells suffer destruction by necrosis leading to diabetogenicity. ROS inactivates the signal pathway between the glucose transporter system and insulin receptor, functioning as a mediator of β -cell dysfunction and insulin resistance [5]. Thus, rodent and pancreatic b cells models are widely used to explore the mechanisms altered in type 2 diabetes [6].

Selenium (Se) has been recognized as a dietary antioxidant and is included in selenocysteine, an amino acid used to synthesize selenoenzymes, whose activity depends on the presence of selenium in their active site. Se in experiments in vitro and in vivo demonstrated insulin-like influence in glucose regulation and protection against reactive oxygen species (ROS), and is important for pharmacological effects and physiological functions [7]. Therapeutic applications of selenium nanoparticles [8]. Selenium nanoparticles (SeNPs) have shown higher biocompatibility and lower toxicity than other inorganic or organic Se compounds, attracting interest for their utilization as therapeutic agents [9]. Selenite possesses strong anti-diabetic properties due to its effect on gluconeogenesis, glycolysis, and fatty acid metabolism [10]. SeNPs are used as nanomaterials because Se(0) can be functionalized/stabilized with different compounds or loaded with specific drugs. SeNPs show physical properties, including the capacity to form distinct shapes associated with the solvents and chemicals used for their synthesis [11].

Several plants worldwide have effect anti-diabetic due to the anti-inflammatory, antioxidant, hypolipidemic, and hypoglycemic activities of the phenolic compounds contained [12]. Flavonoids are natural dietary compounds widely distributed in fruits and vegetables, attracting interest for their lack of toxicity and potential as effective chemopreventive agents against obesity and T2DM [13]. Among these naturally occurring flavonoids, Naringenin (NAR) and Baicalin (BAI) have been evaluated for their potential in the management of diabetes. Naringenin (4,5,7-trihydroxy-flavanone) is found predominantly in citrus fruits. NAR significantly increased glucose uptake and 5'AMP-activated protein kinase (AMPK) phosphorylation/activation [14]. Naringenin treatment on immature 3T3-L1 cells reduces lipid accumulation and inhibits the protein expression of STAT5A, PPAR γ , aP2, and adiponectin, all involved in adipogenesis [15]. NAR in STZ/nicotinamide-induced diabetes reduced triglyceride levels, total cholesterol, and blood glucose, attenuated oxidative stress, hyperglycemia, and increased serum insulin levels [16]. Baicalin decreases postprandial and fasting insulin, glucose, low-density lipoprotein (LDL), triglycerides levels, and tumor necrosis factor-alpha (TNF- α) expression [17], attenuates glucose tolerance and sensibility of insulin [18], increases SOD, CAT, and GPx in the liver, plasma, and pancreas [19].

Until today, no cure for type 2 diabetes has been found; the success of treatment should be focused on the regeneration of destructed β -cells, insulin resistance, and its complications,

including peripheral neuritis and hyperlipidemia, among others. The purpose and the novelty of this investigation are trying to find a mechanism of action of the anti-diabetic effect of a combination of flavonoids (Naringenin and Baicalin) with selenium (NAR/BAI/SeNPs) determining the role of these nanoparticles with hypolipidemic, antioxidant, β -cells regenerative and insulin resistance results on STZ-induced diabetic mice using biochemical parameters and INS-1 pancreatic β -cells.

2. Materials and Methods

2.1. Green synthesis of Se-conjugated with NAR and BAI.

The nanoparticles were synthesized using the sol-gel method with $\text{Na}_2\text{Se}_2\text{O}_3$. An aqueous solution containing 100 mM sodium selenite, 50 mg of NAR, and 50 mg of BAI was added dropwise, and an aqueous solution containing 100 mg of ascorbic acid as a reducer. After the addition of the reductant, the solution turned orange-red. The reaction proceeded for 6 h with an agitation speed of 600 rpm before the nanoparticles were collected by centrifugation at 12,000 rpm at 15 min to remove the excess sodium selenite and other precursors. Then NPs were washed twice with Milli-Q water. The solution containing NAR/BAI/SeNPs was dialyzed against distilled water for 24 h and stored at room temperature.

2.2. Characterization.

The morphology of NAR/BAI/SeNPs was investigated using a high-resolution transmission electron microscope (TEM; Model HT7700, Hitachi High-Tech, Tokyo, Japan). The zeta potential of nanoparticles and particle size were measured by using laser Doppler velocimetry (LDV, Zetasizer Nano ZS, Malvern, UK). Dynamic light scattering (DLS) was used to monitor particle size changes during storage in a Zetasizer Nano ZSP, Malvern Instruments Ltd., Malvern, UK. The FT-IR spectra of NAR/BAI and NAR/BAI/SeNPs were characterized by using a spectrophotometer FTIR-TENSOR27, Bruker, Ettinger, Germany, in the range of $400\text{--}4000\text{ cm}^{-1}$.

The UV-visible spectra were obtained using a UV-250 Shimadzu spectrophotometer in Tokyo, Japan. The 525 absorbances were determined in the range of 250–700 nm. The elemental compositions of the NAR/BAI/SeNPs were measured by using Energy-dispersive X-ray spectroscopy (EDS) by SEM-EDX spectrometer (Oxford Ltd, UK).

2.3. Encapsulation efficiency (EE) and loading content (LC).

EE is defined as the real content of the drug loaded into the nanoparticles. 20 mg of freshly prepared NAR/BAI/SeNPs was centrifuged at 9000 rpm for 30 min at room temperature. The supernatant was analyzed for NAR/BAI using UV-vis spectrophotometry at 360 nm. To determine the EE, the initial amount of NAR/BAI was equal to its loaded content with nanoparticles, and free NAR/BAI (in supernatant, no loaded NAR/BAI) was determined. The EE and LC were calculated using Equations (1) and (2), respectively.

$$EE = \frac{\text{Initial amount of NAR/BAI} - \text{Free NAR/BAI} \times 100}{\text{Initial amount of PPE}} \quad (1)$$

$$LC = \frac{\text{Initial amount of NAR/BAI} - \text{Free NAR/BAI}}{\text{Mass of carrier (CSNPs)}} \times 100 \quad (2)$$

2.4. *In vitro* NAR/BAI release from NAR/BAI/SeNPs

The *in vitro* NAR/BAI release assays were carried out on simulated gastrointestinal tract conditions [20]. Twenty mg of NAR/BAI/SeNPs was added to 40 mL of simulated gastric fluid [SGF, 8.0g/L pepsin, 0.02 g/L ammonium bicarbonate (NH₄HCO₃), 0.01 g/L magnesium chloride hexahydrate (MgCl₂·6H₂O), 1.38 g/L sodium chloride (NaCl), 1.05 g/L sodium bicarbonate (NaHCO₃), 0.06 g/L potassium dihydrogen phosphate (KH₂PO₄), and 0.26 g/L potassium chloride (KCl); at pH 3.0] or simulated intestinal fluid [SIF, 2.5 g/L pancreatin, 6.3 g/L bile salts, 0.03 g/L magnesium chloride (MgCl₂), 1.12 g/L sodium chloride (NaCl), 3.75 g/L sodium bicarbonate (NaHCO₃), 0.05 g/L potassium dihydrogen phosphate (KH₂PO₄), 0.25 g/L potassium chloride (KCl); at pH 7.0]. The solutions were placed in different Eppendorf tubes divided into equal volumes, then Eppendorf tubes were incubated at 37°C in a water bath shaker at 100 rpm/min. After 0, 1, 2, 3, 4, 5, 6, 7, 8, 9, and 10 hours, a tube was taken out and quantified using UV-vis spectrophotometry at 360 nm. Cumulative release (%) was calculated using Equation (3).

$$\text{Cumulative release \%} = \frac{\text{released NAR/BAI}}{\text{total NAR/BAI}} \times 100 \quad (3)$$

2.5. *Animals*

Adult C57BL/6 mice (male) of about eight weeks old were utilized in this study. All the mice were provided with free access to water and food. The experiments reported in this study followed the guidelines stated in "Principles of Laboratory Animal Care" (NIH publications 85-23, revised 1985) and Mexican Official Normativity (NOM -062-Z00-1999). Then obtaining approval from the Institutional Animal Care and Animal Experiment Committee of Escuela Nacional de Ciencias Biológicas, IPN approved all animal experiments (Code: Folio ENCB/CEI/046/2021).

2.6. *Induction of diabetes in mice.*

A fresh streptozotocin (STZ) solution was prepared immediately before an intraperitoneal injection (i.p.), in 0.05 M concentration of citrate buffer of pH 4.5. Diabetes was induced in C57BL/6 mice with a dose of 50 mg/kg body weight [BW] for 5 consecutive days. The blood drops were collected from the tail every week to measure the blood glucose levels using an Accu-check blood glucose meter. The mice were considered hyperglycemic, with blood glucose levels equal to or greater than 250 mg/dl (13.9 mM) after 7 days of STZ administration.

2.7. *Experimental design.*

Forty-two male C57BL/6 mice were divided into 6 groups. The detail of the experimental groups is as follows:

Group 1: operate as normal control, was injected i.p. with citrate buffer
Group 2: mice were injected i.p. with STZ (50 mg/kg b.wt. for 5 consecutive days) for induction of diabetes and reserved as a positive control group.

Group 3: mice with STZ induce-diabetes were treated with NAR/BAI mixture at a dose (10mg/kg/day) given as 0.5 ml orally by intra-gastric tube daily for 8 weeks. Group 4: mice with STZ induce-diabetes were treated with SeNPs at a dose (10mg/kg/day) given as 0.5 ml orally by intra-gastric tube daily for 8 weeks. Group 5: mice with STZ induce-diabetes were treated with NAR/BAI/ SeNPs at a dose (10mg/kg/day) given as 0.5 ml orally by intra-gastric tube daily for 8 weeks. Group 6: mice with STZ induce-diabetes were treated with Metformin (Mtf) at a dose (150mg/kg/day) given as 0.5 ml orally by intra-gastric tube daily for 8 weeks. Changes in the Body weight (g) of mice in all groups were measured and recorded every week.

2.8. Biochemical analysis of serum of diabetic mouse.

At the end of the experiment, all mice were sacrificed, blood was collected, and serum was separated immediately. Glucose level, insulin level, HbA1c, Total Cholesterol (TC), Triacylglycerols (TG), High-density lipoprotein-cholesterol (HDL-c), Low-density lipoprotein-cholesterol (LDL-c), Non-esterified fatty acids (NEFA) were determined used ELISA kit (Thermo-Fisher Scientific, Waltham, MA, USA). HOMA-IR was calculated according to existing literature formulas [21].

2.9. Oral glucose tolerance test (OGTT) and insulin tolerance test (ITT).

At week 8, all mice fasted for 12 hours with the free from water prior to OGTT. C57BL/6 mice were administrated as 0.5 ml orally by an intra-gastric tube with a glucose solution (2 g/kg). While at the 8th week, all mice were fasted and free from water for 4 hours before the ITT was intraperitoneally injected with insulin (1 U/kg, Sigma-Aldrich, St. Louis, Mi, USA). In OGTT and ITT methods, the blood glucose levels were detected at 0, 30-, 60-, 90, 120- and 150- min after the glucose, or insulin, was administrated to the mice.

2.10. Assessment of antioxidant enzymes, lipid peroxidation (LPO), and transaminases ALT, AST, ALP.

At the end of the treatment of 8 weeks with NPs, the animals were fasted overnight, after which they were sacrificed by cervical dislocation and necropsied. The liver was removed surgically, homogenized in PBS to prepare 10% liver homogenate after centrifugation (3500 rpm, 15 min, 4° C), and the supernatant was collected. The content of MDA, antioxidant enzymes CAT SOD, GPx, transaminases, AST, ALT, and ALP in the supernatant of liver homogenate were measured according to the instructions provided in Elisa kit assays (Ela science, CA, USA).

2.11. Liver and muscle glycogen determination.

Liver or muscle glycogen content was determined using 5 μ L of amyloglucosidase, sodium acetate buffer (100 μ L; pH 6), and 20 μ L of the liver or muscle homogenate to a final volume of 0.5 mL. A control without amyloglucosidase was also investigated. 1 mL of glucose oxidase/peroxidase reagent (GOPOD, 626 Megazyme) was added to 300 μ L aliquot of each sample and incubated at 50 °C for 30 min. Then based on a calibration curve constructed by reacting D-glucose with several concentrations of GOPOD reagent, the glycogen content was evaluated at 510 nm.

2.12. Cell culture.

INS-1 pancreatic β -cells (insulinoma pancreatic b cells) were obtained from ATCC; cultured in RPMI 1640 medium, supplemented with penicillin (100 units/ml), 10 % fetal bovine serum (FBS), and streptomycin (100 μ g/ml) at 37 °C in a humidified atmosphere containing 5 % CO₂. The medium was modified every day till the cells grew to a confluency of 70%.

2.13. Cell viability.

Cell viability was investigated by a colorimetric MTT assay, based on the conversion of MTT to MTT-formazan by mitochondrial enzymes.²¹ INS-1 pancreatic β -cells (2 \times 10⁴ cells/well) were seeded in wells of 96-well plates and let adhere overnight. After INS-1 cells were cultured in RPMI-1640 medium and preincubated with normal glucose levels (11mM) or high glucose levels (30mM) for 48 h, and after incubated in the absence or presence of NAR/BAI/SeNPs (0.0125, 0.025, 0.05, 0.1, and 0.2 mg/mL) for 24 h. After the experimental time period, 100 μ l of MTT solution (1 mg/ml) was added to each well of the 96-well culture plate, and incubated for an additional 4 h at 37 °C. Then added 100 μ l DMSO for solubilized formazan crystals. Absorbance was measured at 540 nm using a microplate reader (Sunrise, Tecan, Salzburg, Austria). Cell viability (%) was calculated using equation 4:

$$\text{Cell viability (\%)} = \frac{\text{Absorbance of the sample} \times 100}{\text{Mean absorbance of the 11:1 mM glucose and non-treated control.}} \quad (4)$$

2.14. Determination of glucose-stimulated insulin secretion in INS-1 pancreatic β -cells

INS-1 pancreatic β -cells were pre-incubated with glucose (5.5 mM or 30 mM) for 48 h, and incubated with or without nanoparticles for 48 h. The medium was eliminated, and the cells were washed with PBS, before a fresh medium constituted with 2% FBS and 3 mM glucose was introduced. After being incubated for 5 h, the cells were stimulated with Krebs-Ringer buffer (20 mM HEPES, 5 mM NaHCO₃, 1.2 mM KH₂PO₄, 1.2 mM MgSO₄, 2.54 mM CaCl₂, 4.75 mM KCl, 119 mM NaCl with pH 7.4) and glucose (11mM or 30 mM), incubated for 60 min at 37 °C. After the medium was collected and insulin secretion was determined, used ELISA kit.

2.15. Statistical analysis.

Results were shown as mean \pm SD (n=20). Statistical analysis was carried out at p < 0.05 between the groups by one-way analysis of variance (one-way ANOVA) and by Tukey's multiple comparisons

3. Results and Discussion

3.1. Synthesis of NAR/BAI/ SeNPs.

The synthesis of SeNPs was performed by the reduction of sodium selenite (+IV oxidation state) to elemental selenium by ascorbic acid. The color of the reaction mixture was pale yellow at the initial point of reaction, which gradually is modified to orange-red (Figure 1A); this color was associated with the excitation of surface plasmon of the Se nanoparticles, indicating that SeO₃ is reduced to Se⁰. The surface plasmon showed a characteristic absorption peak at 270 nm (Figure 1B); our results agree with other investigations on SeNP synthesis [23].

The spectra of UV absorption indicated that flavonoids were successfully absorbed on the surface of nanoparticles, as shown in Figure 1C, which correspond to the spectra of NAR/BAI combination and NAR/BAI/SeNPs.

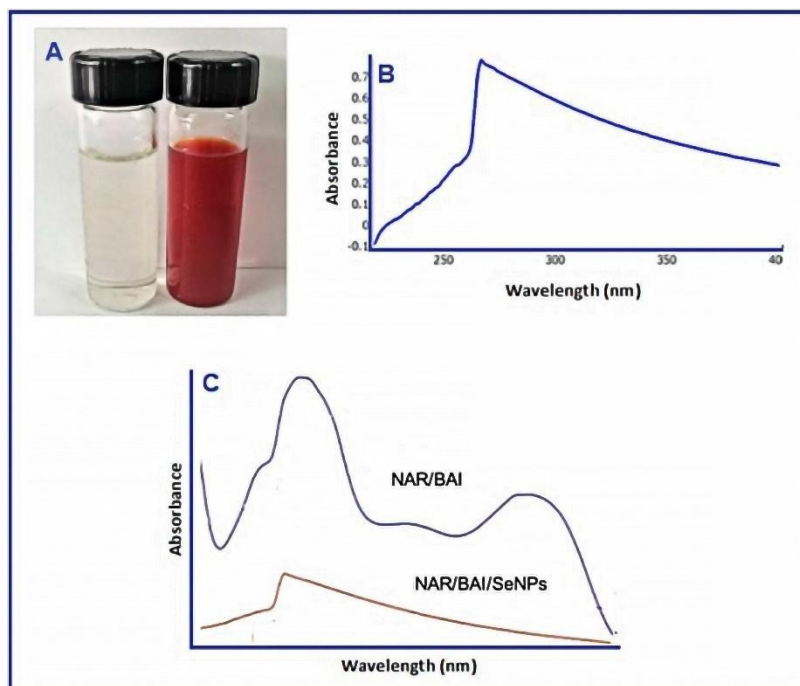


Figure 1. (A) Formation of SeNPs synthesized with BSA; (B) UV-Visible spectrum for selenium nanoparticles (SeNPs); (C) NAR/BAI mixture, and NAR/BAI /BSA-SeNPs from 200 to 800nm.

3.2. Fourier transformer infrared spectrophotometer (FTIR) analysis.

FTIR study was carried out to characterize the surface chemistry of selenium nanoparticles with flavonoids. The bands observed at 1648, 1610, and 1521 cm^{-1} supported the presence of carbonyl groups in the structure of the flavonoids (Figure 2). The other intensive band at 858 cm^{-1} was generated by the deformation of C-OH and C-O groups variation from the structure of combined flavonoids.

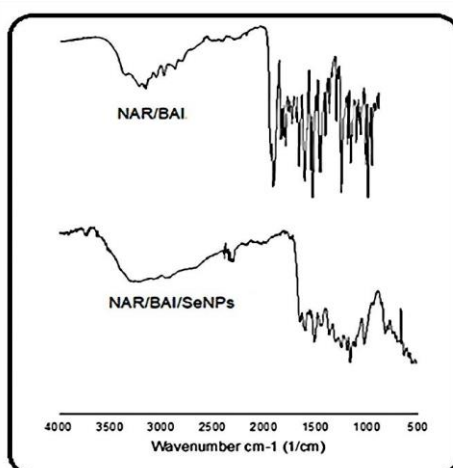


Figure 2. FTIR spectra: NAR/BAI mixture and NAR/BAI / SeNPs.

However, The FTIR spectra of the combination of NAR/BAI indicated a broad band at 3284 cm^{-1} generated from the valence vibration of (O-H) groups in the structure of compounds, associated with the formation of intramolecular hydrogen with the carbonyl (C=O) group of the ring. Figure 2 shows the absorption peaks at 1650 and 1555 cm^{-1} , characteristic of C-H

vibrations of flavonoids surrounding the selenium nanoparticles (Figure 2). The FTIR of the NAR/BAI/SeNPs spectrum showed bands at 3430 and 3050 cm^{-1} related to O-H stretching vibration. The hydroxyl groups of icariin and hesperidin interacted with SeNPs forming a stable structure.

3.3. Physicochemical properties.

The zeta potential and size distribution of the NPs were measured by dynamic light scattering. NAR/BAI/SeNPs showed a size distribution of 80 nm and 119 nm with an average diameter of 104.9 nm (Figure 3A) and displayed a zeta potential of -22.3 mV, which indicated that the nanoparticle system easily could interact with flavonoids due to the positive charge of SeNPs surface. The polydispersity index (PDI) observed was 0.249 indicating the low aggregation of particles. This PDI was below 0.3, which demonstrated that flavonoids-conjugated with Se (Figure 3B). The size distribution of SeNPs was also measured, indicating an average diameter of 47.84 nm and 80.23 nm, respectively, supporting that flavonoids were loaded and Se surface decoration increased narrow size distribution. The size distribution of NAR/BAI/SeNPs was further confirmed by TEM (Figure 3C), which showed that NPs were spherical and well dispersed. Findings indicated that the average diameters were higher than those obtained by TEM assay, possibly because of the flavonoid molecule on the surface of the NPs and the water molecules around the nanoparticles, forming a hydrodynamic radius [23].

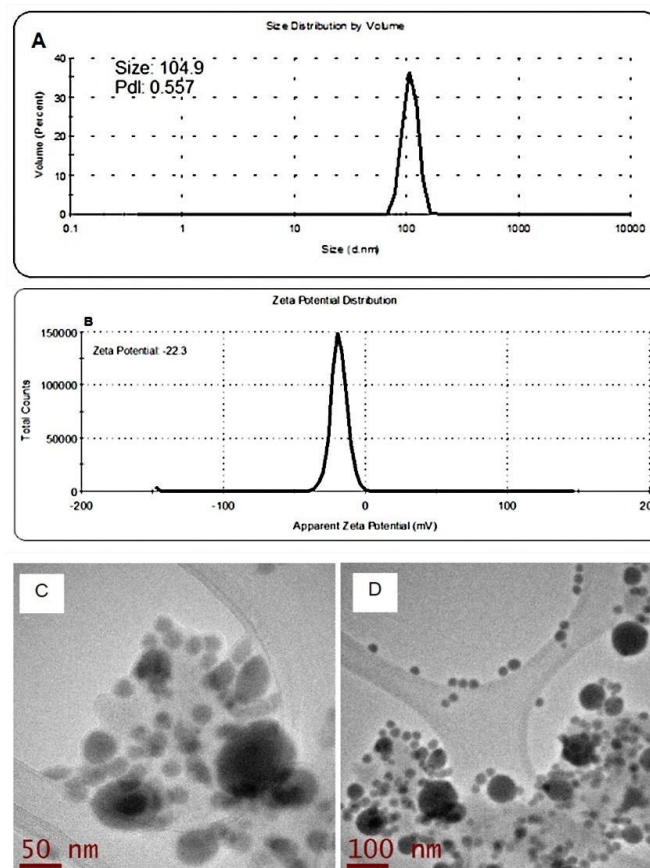


Figure 3. DLS analysis of synthesized NAR/BAI /BSA-SeNPs (A); zeta potential measurement (B); transmission electron microscope (TEM) images of NAR/BAI /BSA-SeNPs (C)

In addition, this investigation described the elemental compositions of the SeNPs (Figure 4A) and NAR/BAI/SeNPs (Figure 4B). The EDX spectrums showed the carbon, oxygen, and selenium signals indicating the presence of flavonoids on the surface of the SeNPs. EDX does not show other significant impurity peaks. The results demonstrate that the nanoparticles of selenium in the presence of flavonoids were successfully synthesized.

3.4. Encapsulation efficiency and loading content and stability.

Findings indicated that encapsulated icariin and hesperidin internal nanoparticles (EE) content was 80.1% while LC was 25.4%, indicating good physical stability and high encapsulation efficiency and loading capacity. In addition, NAR/BAI/SeNPs remained stable over a storage period of almost 6 months without any aggregation and precipitation observed at this time (Fig. 4 C).

3.5. In vitro release of naringenin and baicalin.

Naringenin and baicalin combination release from nanoparticles was performed at pH of 3.0 and 7.0 at 37°C, which was described with an initial fast release followed by a slower and gradual flavonoid release (Fig. 4D). The initial release from the first minutes, possibly results from the desorption of surface-bound nanoparticles. The release continues at a slower rate till it achieves a plateau at 6 h.

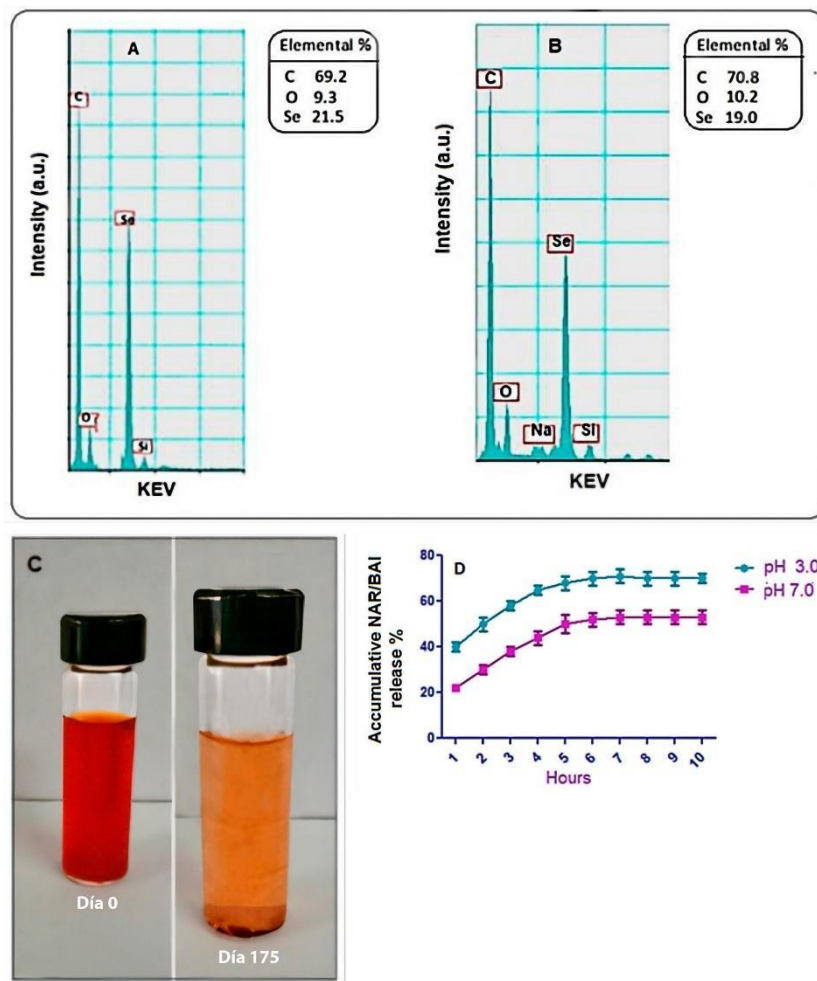


Figure 4. Energy dispersive X-ray spectroscopy of SeNPs (A); The surface elemental compositions by energy-dispersive X-ray (EDX) of NAR/BAI/BSA-SeNPs (B); Photographs of NAR/BAI/BSA-SeNPs during a 175 days period (C); In vitro release of NAR/BAI from NAR/BAI/BSA-SeNPs at pH 3 and pH 7.0 (D)

This research proposes new appreciation using integrative nanomedicine containing flavonoids and selenium for diabetes mellitus type 2 treatment to those in the chemical drug Metformin which is used as an oral hypoglycemic agent.

3.6. Effects on body weight.

The body weight changes for the animal groups through the 8 weeks of treatment are displayed in Table 1. Results indicated that Group-2 experienced a weight loss of up to 13.3% after 8 weeks while Groups 3, 4, and 5 not only detain its reducing trend but also produced an increase of 12.5%, 9%, and 14%, respectively. Mtf-treated Group 6 showed an increase of up to 4.6% less than that of other Groups. Findings demonstrated a trend of weight gain in Group-3 and Group-5 compared to Group-4 (SeNPs control). Treatment of nanoparticles enhances this body weight decrease in T2DM and healthy mice.

T2DM is associated with body weight loss, reduction of tissue protein, and muscle wasting as a result of insulin deficiency and insulin resistance [24]. Thus, weight reduction is a result of the progressive impairment of insulin effect in diabetes, reducing in the skeletal muscle the influx of amino acids to increase protein synthesis [25]. Our findings indicated that administering NAR/BAI/SeNPs was effective against overage body weight loss in diabetic mice.

Table 1. Effect of normal control (Group-1), diabetic control group (Group-2), diabetic treated with NAR/BAI mixture (Group-3), diabetic treated with SeNPs (Group-4), diabetic treated with NAR/BAI/SeNPs (Group-5), and diabetic treated with Mtf (Group-6), on the changes of diabetic mice body weight, (mean ± SD) through 8 weeks of experimentation.

Body weight (g)						
Week	Group-1	Group-2	Group-3	Group-4	Group-5	Group-6
0	25.3± 3.4	26.3± 2.7	24.7± 0.9	27.6± 2.5	26.4± 1.8	27.8± 3.1
1	25.8± 2.9	25.8± 3.1	24.7± 4.3	27.9± 4.3	27.9± 2.3	26.0± 1.0
2	26.3± 3.4	25.1± 2.9	25.2± 3.7	28.2± 3.7	28.2± 0.9	26.5± 0.9
3	26.5± 4.0	24.2± 1.1	25.6± 2.8	28.7± 2.8	28.7± 2.1	27.0± 0.8
4	26.7± 1.7	24.7± 1.5	25.8± 3.4	29.4± 3.4	29.4± 3.0	28.4± 1.1
5	26.9± 3.6	23.2± 2.6 ^a	26.3± 2.5	29.6± 2.5	29.6± 2.4	28.4± 0.7
6	27.0± 3.8	23.9± 3.0 ^c	26.7± 4.1	29.8± 4.1	29.8± 1.5	28.5± 1.2
7	27.1± 1.8	22.0± 2.8 ^a	27.0± 4.3 ^{**}	30.0± 4.3 [*]	30.0± 1.7 ^{##**}	29.0± 1.5
8	27.3± 3.4 (↑7.9%)	22.8± 2.3 ^b (↓13.3%)	27.8± 2.2 ^{##**} (↑12.5%)	30.1± 4.2 [*] (↑9.0%)	30.1± 3.1 ^{##*} (↑14.0%)	29.1± 0.7 (↑4.6%)

Data are expressed as mean ± SD. *p<0.05 and, **p<0.01 vs diabetes group; ap<0.05, bp<0.01 and, cp<0.001 vs control group (n=7 for each group). #p<0.05 vs SeNPs group

3.7. Hematological changes in type 2 diabetes mellitus mice (T2DM).

To measure the effect of SeNPs, NAR/BAI, and NAR/BAI/SeNPs on fasting glucose levels and insulin levels were evaluated in plasma. As shown in Table 2, fasting blood glucose, insulin levels, HOMA-IR, and HbA1c levels significantly increased in diabetic mice. While these parameters were significantly reduced by the daily administration of SeNPs, NAR/BAI, and NAR/BAI/SeNPs for 8 weeks, improvement of the status of insulin resistance, and HOMA-IR, ameliorates the progression of hyperglycemia and HbA1c showed a significant decrease when compared to the diabetic group.

The animals displayed a normal basal blood glucose level before treatment with STZ. However, then 7 days of STZ administration, the mice indicate a significant increase in their

blood glucose level. Oral treatment of NAR/BAI/SeNPs decreases blood glucose levels in T2DM mice, similar to that observed in the metformin group.

Serum insulin levels significantly ($p < 0.05$) decreased in the diabetic group associated with the capacity of STZ in the production of ROS and rapid depletion of beta cells [26], causing hyperglycemia and the development of diabetic complications. However, results of insulin levels in diabetic mice suggested that a few healthy β -cells remained to generate some insulin. Whereas glucose level was increased in diabetic mice, the nanoparticles exhibited good efficacy in controlling and fasting blood glucose levels in diabetic mice over a period of 8 weeks. Findings indicated that NAR/BAI/SeNPs increase serum levels of insulin and consequently reduce blood glucose in treated diabetic mice.

HOMA-IR showed a significant reduction after treatment with NAR/BAI/SeNPs, reflecting an anti-diabetic effect via ameliorated β -cell function and insulin sensitivity. HbA1c level indicates the average blood glucose concentration in the past 1–2 weeks [27]. The diabetic mice treated with nanoparticles showed HbA1c nearby normal levels as a consequence of ameliorated glycemic control produced by the initiation of the glycogen generation framework of nanoparticles. Thus, the reduction of HbA1c showed the capacity of NAR/BAI/ SeNPs to control T2DM [28]. NAR/BAI/ SeNPs had a greater effect than those produced by NAR/BAI, and SeNPs suggested that this effect can be for the synergic effect of flavonoids and selenium. The protective effect of NAR/BAI/SeNPs in hyperglycemia conditions could be related to a decrease in blood glucose level and stimulated glucose uptake by peripheral tissues, stimulating insulin secretion.

Table 2. Effect of nanoparticles on fasting blood glucose levels, insulin, HbA1C, and HOMA-IR in plasma.

Groups	Glucose (mg/dl)	Insulin (μ U/mL)	HOMA-IR	HbA1C (mg/g Hb)
1 (normal)	94 \pm 4.17	17.6 \pm 2.16	3.38 \pm 1.98	0.28 \pm 0.-01
2 (diabetic control)	230 \pm 6.23 [#]	11.8 \pm 1.54 ^{##}	6.60 \pm 3.47 [#]	0.79 \pm 0.-04
3 (Diabetic + NAR/BAI)	125 \pm 3.87 ^{##}	16.2 \pm 2.31 ^{##}	4.98 \pm 3.48 ^{###}	0.35 \pm 0.-02 ^{##}
4 (Diabetic + SeNPs)	148 \pm 6.54 ^{###}	12.6 \pm 1.54	4.59 \pm 2.14 ^{###}	0.44 \pm 0.-01 ^{#####}
5 (Diabetic + NAR/BAI/ SeNPs)	86 \pm 4.98 [*]	18.3 \pm 1.76 ^{**}	3.87 \pm 2.14 [*]	0.26 \pm 0.-03 ^{**}
6 (Diabetic + Mtf)	102 \pm 5.72 ^{**}	16.4 \pm 3.05 [*]	4.12 \pm 2.14 ^{###}	0.30 \pm 0.-04 [*]

Data are expressed as mean \pm SD; (n=7). ^{***} $p < 0.001$, ^{**} $p < 0.01$ and, ^{*} $p < 0.05$, vs diabetes group; [#] $p < 0.05$ and, ^{##} $p < 0.01$ vs control group

3.8. Effect on insulin resistance induced by ZTZ in C57BL/6J mice.

The oral glucose tolerance test (OGTT) and Insulin tolerance test (ITT) were carried out over 8 weeks. OGTT experiment in mice is a widely accepted assay to evaluate insulin resistance and peripheral insulin action in animals. As shown in Table 3, the OGTT of diabetic mice induced-STZ showed insulin tolerance and impaired glucose. Both NAR/BAI and NAR/BAI/SeNPs treatment enhance insulin and glucose tolerance better than the SeNPs group. NAR/BAI/ SeNPs showed a significant decrease effect when compared to the Metformin group. However, ITT is useful for assessing insulin sensitivity by exogenous insulin administration. As shown in Table 3, the ITT of diabetic mice induced-STZ showed impaired glucose.

NAR/BAI/SeNPs decrease the blood glucose significantly at 30 min of administration, indicating an ameliorated insulin sensitivity in mice, possibly by enhancing insulin receptors such as insulin receptor substrate, namely insulin receptor, or also improving the enzymes involved in phosphorylation of glucose and glucose transporters [29]. Findings of OGTT and ITT established that NAR/BAI and NAR/BAI/SeNPs treatment decrease glucose levels,

possibly using the mechanism of insulin-sensitized glucose uptake [30], supporting that NAR/BAI, and NAR/BAI/SeNPs can improve insulin resistance status in T2DM mice. Oral administration of nanoparticles significantly enhances insulin resistance and insulin level showing the insulin secretagogue effect for the disposal of blood glucose levels [16].

Table 3. Effect of SeNPs, NAR/BAI, and NAR/BAI/SeNPs on OGTT
Fasting blood glucose levels (nmol/L)

Group	0	30 min	60 min	90 min	120 min	150 min
Group-1	5±1.73	12±1.0	10±0.56	8± 2.10	7±0.86	5±0.87
Group-2	18±1.54	31±4.26	29±0.78	25±5.04	20±0.87	17±1.64
Group-3	16±2.76	33±4.12	26±0.76*	20±4.62**	16±1.01***	13±1.12*#
Group-4	13±1.48	30±1.98	27±0.34	20±5.23**	17±1.24**	15±2.11
Group-5	15±3.00	28±4.54	22±0.51**	17±1.16*#	13±1.67*#	10±1.78*#
Group-6	12±2.16	29±1.87	24±0.45*	19±2.54*	15±0.93***	12±1.56*#

Values indicate mean ± standard error of the mean (SD of seven mice per group). *p < 0.005

**p < 0.001, compared with diabetic control values. #p<0.05 vs SeNPs group

3.9. Effect on dyslipidemia.

Table 3. Effect of SeNPs, NAR/BAI, and NAR/BAI/SeNPs on OGTT.
Fasting blood glucose levels (nmol/L)

Group	0	30 min	60 min	90 min	120 min	150 min
Group-1	5±1.73	12±1.0	10±0.56	8± 2.10	7±0.86	5±0.87
Group-2	18±1.54	31±4.26	29±0.78	25±5.04	20±0.87	17±1.64
Group-3	16±2.76	33±4.12	26±0.76*	20±4.62**	16±1.01**#	13±1.12*#
Group-4	13±1.48	30±1.98	27±0.34	20±5.23**	17±1.24**	15±2.11
Group-5	15±3.00	28±4.54	22±0.51**	17±1.16*#	13±1.67*#	10±1.78*#
Group-6	12±2.16	29±1.87	24±0.45*	19±2.54*	15±0.93***	12±1.56*#

Values indicate mean ± standard error of the mean (SD of seven mice per group). *p < 0.005 and **p < 0.001, compared with diabetic control values. #p<0.05 vs SeNPs group

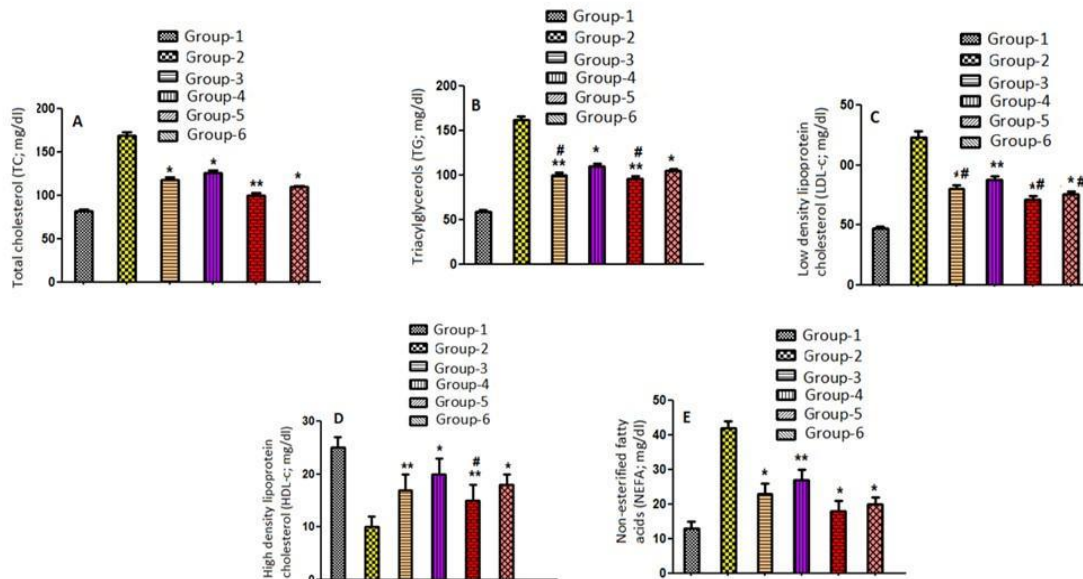


Figure 5. Effect of normal control (Group-1), diabetic control group (Group-2), diabetic treated with NAR/BAI mixture (Group-3), diabetic treated with SeNPs (Group-4), diabetic treated with NAR/BAI/BSA-SeNPs (Group-5), and diabetic treated with Mtf (Group-6), Total Cholesterol (TC) (A); Triacylglycerols (TG) (B); Low-density lipoprotein-cholesterol (LDL-c) (C); High-density lipoprotein-cholesterol (HDL-c) (D); Non-esterified fatty acids (NEFA)(E) in 8 weeks of experimentation. Data are expressed as mean ± SD (n=7 for each group). *p<0.05 and, **p<0.01 vs diabetes group. #p<0.05 vs SeNPs group.

The diabetic condition produces profound alterations in lipid profile development dyslipidemia. In the present study, group 2 (diabetic control) for 8 weeks showed an expected increase of TC, TG, LDL-c, and NEFA and reduced HDL-c in serum compared to the corresponding controls (Figure 5A-E). In diabetes mellitus, change in lipid metabolism is associated with insulin resistance, insulin deficiency, and increased flux of free fatty acids in the liver leading to fatty acid accumulation, mainly of triglycerides. The increased triglyceride levels reduce the concentration of HDL-c and the level of LDL-c by activating lecithin acyl-cholesterol transferase and lipoprotein lipase [31]. The increased lipid levels lead to the exaggerated production of ROS, leading to a destabilization of membrane lipids [32]. Administration of NAR/BAI, SeNPs, and NAR/BAI/SeNPs for 8 weeks to diabetic mice shows a significant restoration in impaired lipid profile.

3.10. Determination of antioxidant status.

Antioxidant defense decreases in diabetes; thus, in experimental STZ-mice-induced T2DM, lipid peroxidation is accompanied by significantly decreasing antioxidative enzymes SOD, CAT, and GPx to those in the normal mice. When T2DM mice were treated with NAR/BAI, SeNPs, and NAR/BAI/SeNPs antioxidant capacity of SeNPs was lower than that of NAR/BAI and NAR/BAI/ SeNPs. However, NAR/BAI/SeNPs significantly increase the activity of antioxidative enzymes SOD, CAT, and GPx (Figure 6A-D). The formation of malondialdehyde produces lipid peroxidation causing cross-linking polymerization of several macromolecules. LPO is favored by hyperlipidemia and hyperglycemia [33] so the malonaldehyde (MDA) content is higher than that of diabetic mice.

In diabetes, different mechanisms may produce an increase in oxidative stress. Chronic hyperglycemia can increase the production of free radicals due to the capacity of the glucose to enolize and generate oxidizing intermediates, including hydrogen peroxide (H₂O₂), nitric oxide (NO), hydroxyl radical (-OH), and superoxide anion (O₂⁻) among others [34].

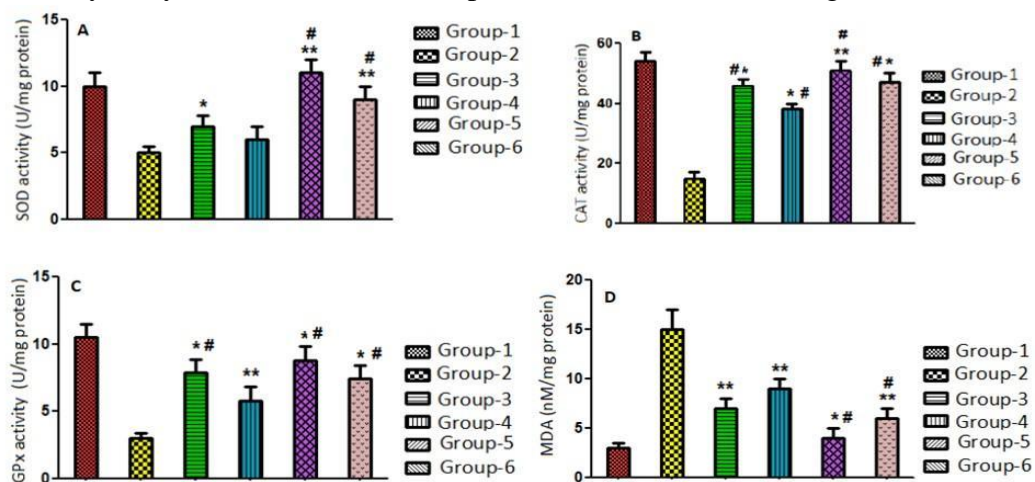


Figure 6. Determination of antioxidant status in normal control (Group-1), diabetic control group (Group-2), diabetic treated with NAR/BAI mixture (Group-3), diabetic treated with SeNPs (Group-4), diabetic treated with NAR/BAI/BSA-SeNPs (Group-5), and diabetic treated with Mtf (Group-6), superoxide dismutase (SOD) (A); Catalase (CAT) (B); glutathione peroxidase (GPx) (C); malonaldehyde (MDA) (D) in 8 weeks of experimentation. Data are expressed as mean ± SD (n=7 for each group). *p<0.05 and, **p<0.01 vs diabetes group. #p<0.05 vs SeNPs group.

NAR/BAI/SeNP reduces the MDA content better than that of the SeNP and NAR/BAI groups. NAR/BAI/SeNPs demonstrated antioxidant capacity established in the upregulation of gene expressions in the antioxidant enzymes SOD, CAT, and GPx, with the consequent

improvement in the removal of reactive oxygen species accompanied by a marked inhibition of LPO, which indicated that treatment with NAR/BAI/BSA-SeNPs promotes antioxidant potential.

3.11. Effect of nanoparticles on serum hepatic marker enzymes.

The results in Figure 7 (A-D), in conjunction with the above, show how the hypoglycemic effect of NAR/BAI/SeNPs affects different organs. Thus, we examined their effects on the liver. Treatment with NAR/BAI/SeNPs displayed a significant amelioration in all biomarker concentrations (ALP, ALT, and AST) to those in the diabetic non-treated mice (Group 2), obtaining similar values compared with Group 1. ZTZ-induced diabetic mice showed damage in the functional, structural liver and hypertriglyceridemia, which accelerates liver fibrosis distinguished by the accumulation of extracellular matrix leads to liver dysfunction [35].

In diabetic animals, high transaminase concentrations (ALP, ALT, and AST) were observed. NAR/BAI/SeNPs reduced transaminase levels suggesting liver function repair. Liver glycogen concentration is used as a biomarker for measuring the anti-hyperglycemic efficiency of a drug in experimental animals. NAR/BAI/SeNPs significantly increased liver glycogen levels demonstrating that they can ameliorate glycolysis by regularizing insulin secretion, also intervene in the control of hepatic glucose generation participating in the control of blood glucose concentration, consequently improving insulin sensitivity in tissue and reducing alterations in lipoprotein and lipid. In summary, NAR/BAI/BSA-SeNPs treatment increases blood glucose transport into the muscle in T₂DM mice.

3.12. Muscle glycogen.

In streptozotocin-induced diabetic mice, muscle glycogen is significantly depleted at 30.76% (Figure 7E). Nevertheless, the insulinotropic effect of NAR/BAI/BSA-SeNPs induced a significant elevation in the glycogen content to those in the normal group stimulating the conversion of intramuscular glucose into glycogen, producing elevated glycogen storage as well as insulin stimulation [36].

3.13. Effects of NAR/BAI/BSA-SeNPs on cell viability of INS-1 pancreatic β -cells.

To measure the cytotoxic effects of nanoparticles on pancreatic β -cells, cell viability was determined using MTT assay. The results exhibited that 0.0125, 0.025, 0.05, 0.1, and 0.2 mg/mL of nanoparticles had no cytotoxic effect on INS-1 cell viability to those in the control group at selected concentrations (Figure 8A). Findings demonstrated that INS-1 pancreatic β -cells treated with NAR/BAI/BSA-SeNPs values from 0.0125 to 0.2mg/mL in normal glucose medium (5.5mM) do not show a cytotoxic effect and increased cell proliferation. Exposure for 48 h of cells to high glucose levels (30mM) significantly reduced cell viability by 25% (Figure 8B).

While NAR/BAI/BSA-SeNPs are able to protect against high glucose-induced damage in INS-1 pancreatic β -cells with viability similar to cells exposed to a normal glucose 5.5mM, it is due to improving insulin function. An increase in normal glucose levels provokes insulin release; instead, chronic exposure of cells to high glucose concentrations results in the disability of insulin secretion and viability [37].

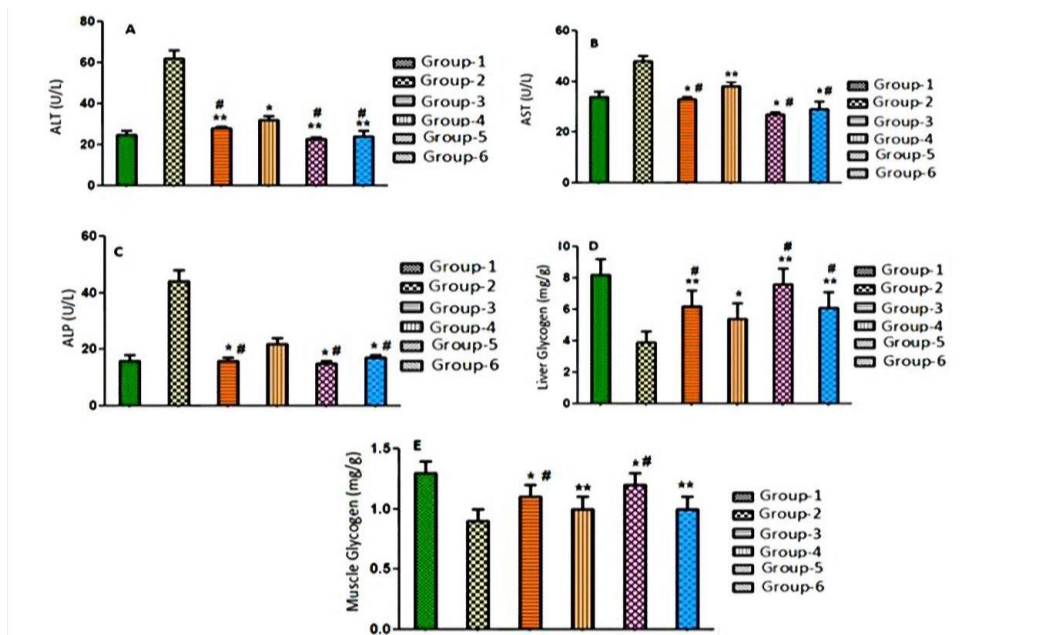


Figure 7. Liver function in normal control (Group-1), diabetic control group (Group-2), diabetic treated with NAR/BAI mixture (Group-3), diabetic treated with SeNPs (Group-4), diabetic treated with NAR/BAI/BSA-SeNPs (Group-5), and diabetic treated with Mtf (Group-6), alanine aminotransferase (ALT) (A); aspartate aminotransferase (AST), (B); alkaline phosphatase (ALP) (C); liver glycogen (D); muscle glycogen (E) in 8 weeks of experimentation. Data are expressed as mean \pm SD (n=7 for each group). *p<0.05 and, **p<0.01 vs diabetes group. #p<0.05 vs SeNPs group

3.14. Effect of nanoparticles on INS-1 pancreatic β cells in insulin secretion.

The insulin secretion of INS-1 pancreatic β cells was markedly reduced in the 30mM glucose treatment compared to those in the 5.5mM glucose treatment (Figure 8C). Thus, the exposure of NAR/BAI/BSA-SeNPs (10, 25, 50 μ g/mL) significantly increased insulin secretion in both treatments.

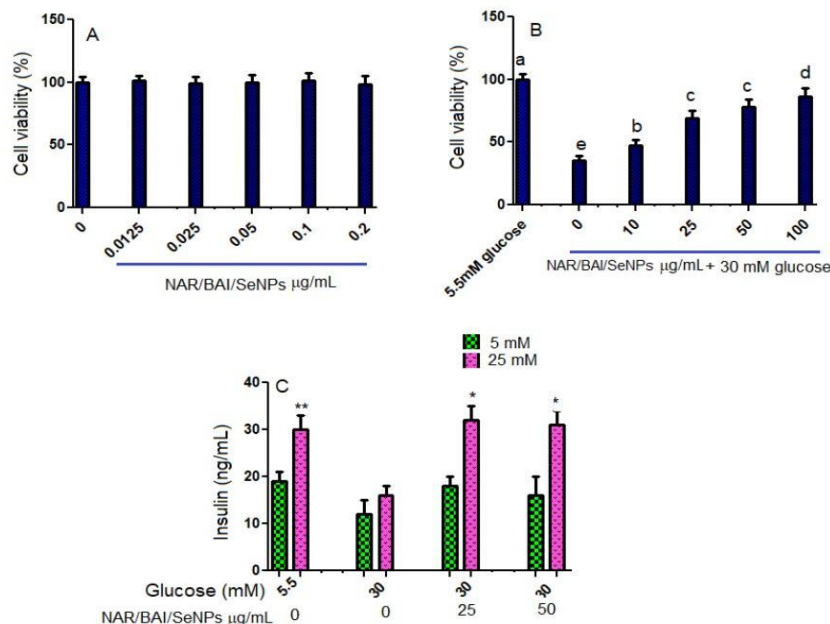


Figure 8. Effect of NAR/BAI/BSA-SeNPs on INS-1 pancreatic β -cells (A) on cell viability; (B) in high glucose-treated INS-1 pancreatic β -cells; (C) on insulin secretion. Each value is expressed as mean \pm SD (n = 3). ^{a-d}different alphabets are significantly different at p < 0.05 and *p<0.01 and **p<0.05 vs high glucose (30 mM).

Results supported the capacity of nanoparticles to improve proliferation, viability, and release insulin secretion in INS-1 cells stimulated under high glucose incubations. Findings demonstrated that nanoparticles increase insulin secretion in INS-1 pancreatic β cells-induced hyperglycemia.

4. Conclusions

This study depicted that NAR/BAI/BSA-SeNPs using an animal model, we found that possess a high efficacy in controlling diabetes with good control of fasting blood glucose level by improving insulin sensitivity, insulin secretion, HbA1c, glucose tolerance, and HOMA-IR index by reinvigorating the β -cells of the pancreas. In contrast, it shows a significant restoration in altered lipid profile. Also, reducing oxidative stress enhances liver glycogen levels due to peripheral glucose utilization and rectifies impaired liver glycolysis. In addition, this investigation demonstrates that NAR/BAI/BSA-SeNPs protect the survival and function of INS-1 pancreatic β cells under glucotoxicity conditions increasing cell viability and insulin secretion. Findings supported that NAR/BAI/BSA-SeNPs can be a potential agent to overcome the impairment of pancreatic β cells associated with type 2 diabetes.

Funding

Financial assistance from the Instituto Politécnico Nacional, CDMX, México is gratefully acknowledged.

Acknowledgments

We appreciate the support provided to the multidisciplinary laboratory for characterization of nanostructures and materials of the IPN.

Conflicts of Interest

The authors declare that they have no known competing financial interests or personal relationships that could have appeared to influence the work reported in this paper.

References

1. Abu-Odeh, A.M.; Talib, W.H. Middle East Medicinal Plants in the Treatment of Diabetes: A review. *Molecules* **2021**, *26*, 742-751, <https://doi.org/10.3390/molecules26030742>.
2. Kumar, S.; Mittal, A.; Babu, D.; Mittal, A. herbal medicines for diabetes management and secondary its complications. *Curr Diabetes Rev.* **2021**, *17*, 437-456, <https://doi.org/10.2174/1573399816666201103143225>.
3. Blahova, J.; Martiniakova, M.; Babikova, M.; Kovacova, V.; Mondockova, V.; Omelka, R. Pharmaceutical drugs and natural therapeutic products for the treatment of type 2 diabetes mellitus. *Pharmaceuticals* **2021**, *14*, 806, <https://doi.org/10.3390/ph14080806>.
4. Rais, N.; Ved, A.; Ahmad, R.; Parveen, K.; Gautam, G.K.; Bari, D.G.; Shukla, K.S.; Gaur, R.; Singh, A.P. Model of streptozotocin-nicotinamide induced type 2 diabetes: a comparative review. *Curr Diabetes Rev.* **2022**, *18*, e171121198001, <https://doi.org/10.2174/1573399818666211117123358>.
5. Mahdavi, A.; Bagherniya, M.; Mirenayat, M.S.; Atkin, S.L.; Sahebkar, A. Medicinal plants and phytochemicals regulating insulin resistance and glucose homeostasis in type 2 diabetic patients: A clinical review. *Adv Exp Med Biol.* **2021**, *1308*, 161-183, <https://pubmed.ncbi.nlm.nih.gov/33861444/>.
6. He, X.; Gao, F.; Hou, J.; Li, T.; Tan, J.; Wang, C.; Liu, X.; Wang, M.; Liu, H.; Chen, Y.; Yu, Z.; Yang, M. Metformin inhibits MAPK signaling and rescues pancreatic aquaporin 7 expression to

- induce insulin secretion in type 2 diabetes mellitus. *J Biol Chem.* **2021**, 297, 101002, <https://doi.org/10.1016/j.jbc.2021.101002>
7. Steinbrenner, H.; Duntas, L.H.; Rayman, M.P. The role of selenium in type-2 diabetes mellitus and its metabolic comorbidities. *Redox Biol.* **2022**, 50, 102236, <https://www.sciencedirect.com/science/article/pii/S2213231722000088>.
 8. Chuai, H.; Zhang, S.Q.; Bai, H.; Li, J.; Wang, Y.; Sun, J.; Wen, E.; Zhang, J.; Xin, M. Small molecule selenium-containing compounds: Recent development and therapeutic applications. *Eur J Med Chem.* **2021**, 5, 113621, <https://doi.org/10.1016/j.ejmech.2021.113621>.
 9. Ferro, C.; Florindo, H.F.; Santos, H.A. selenium nanoparticles for biomedical applications: from development and characterization to therapeutics. *Adv Health Mater.* **2021**, 10, e2100598, <https://doi.org/10.1002/adhm.202100598>.
 10. Zhu, J.; Chen, X.; Li, F.; Wei, K.; Chen, J.; Wei, X.; Wang, Y. Preparation, physicochemical and hypoglycemic properties of natural selenium-enriched coarse tea glycoproteins. *Plant Foods Hum Nutr.* **2022**, 77, 258-264. <https://doi.org/10.1007/s11130-022-00975-2>.
 11. Varlamova, E.G.; Turovsky, E.A.; Blinova, E.V. Therapeutic potential and main methods of obtaining selenium nanoparticles. *Int J Mol Sci.* **2021**, 22, 10808, <https://doi.org/10.3390/ijms221910808>.
 12. Abid, S.; Kaliraj, L.; Rahimi, S.; Kim, Y.J.; Yang, D.C.; Kang, S.C.; Balusamy, S.R. Synthesis and characterization of glycol chitosan coated selenium nanoparticles acts synergistically to alleviate oxidative stress and increase ginsenoside content in Panax ginseng. *Carbohydr Polym.* **2021**, 267, 118195, <https://doi.org/10.1016/j.carbpol.2021.118195>.
 13. Martín, M.A.; Ramos, S. Dietary flavonoids and insulin signaling in diabetes and obesity. *Cells.* **2021**, 10, 1474- 496, <https://doi.org/10.3390/cells10061474>.
 14. Zygmunt, K.; Fauber, B.; MacNeil, J.; Tsiani, E. Naringenin, a citrus flavonoid, increases muscle cell glucose uptake via AMPK. *Biochem Biophys Res Commun.* **2010**, 398, 178–183, <https://doi.org/10.1016/j.bbrc.2010.06.048>.
 15. Richard, A.J.; Amini-Vaughan, Z.; Ribnicky, D.M.; Stephens, J.M. Naringenin inhibits adipogenesis and reduces insulin sensitivity and adiponectin expression in adipocytes. *Evid Based Complement Altern Med.* **2013**, 549750, <https://doi.org/10.1155/2013/549750>.
 16. Annadurai, T.; Muralidharan, A.R.; Joseph, T.; Hsu, M.J.; Thomas, P.A.; Geraldine, P. Antihyperglycemic and antioxidant effects of a flavanone, naringenin, in streptozotocin-nicotinamide- induced experimental diabetic rats. *J Physiol Biochem.* **2012**, 68, 307–318, <https://doi.org/10.1007/s13105-011-0142-y>.
 17. Na, H.Y.; Lee, B.C. Scutellaria baicalensis alleviates insulin resistance in diet-induced obese mice by modulating inflammation. *Intern J Mol Sci.* **2019**, 20, 727, <https://doi.org/10.3390/ijms20030727>.
 18. Waisundara, V.Y.; Hsu, A.; Huang, D.; Tan, B.K. Scutellaria baicalensis enhances the anti-diabetic activity of Metformin in streptozotocin-induced diabetic Wistar rats. *Amer J Chinese Med.* **2008**, 36, 17–540, <https://doi.org/10.1142/S0192415X08005953>.
 19. Shin, N.R.; Gu, H.S.; Kim, H. Combined effects of Scutellaria baicalensis with Metformin on glucose tolerance of patients with type 2 diabetes via gut microbiota modulation. *Amer J Physiol Endocrinol Metab.* **2020**, 318, E52–E61, <https://doi.org/10.1152/ajpendo.00221.2019>.
 20. Stasiak-Różańska, L.; Berthold-Pluta, A.; Pluta, A.S.; Dasiewicz, K.; Garbowska, M. Effect of simulated gastrointestinal tract conditions on survivability of probiotic bacteria present in commercial preparations. *Int J Environ Res Public Health.* **2021**, 18, 1108, <https://doi.org/10.3390/ijerph18031108>.
 21. Matthews, D.R.; Hosker, J.P.; Rudenski, A.S.; Naylor, B.A.; Treacher, D.F.; Turner, R.C. Homeostasis model assessment: Insulin resistance and beta-cell function from fasting plasma glucose and insulin concentrations in man. *Diabetologia* **1985**, 28, 412–419, <https://doi.org/10.1007/BF00280883>.
 22. Selmani, A.; Ulm, L.; Kasemets, K.; Erceg, I.; Barbir, R.; Pem, B.; Santini, P.; Marion, D.; Vinković, T.; Krivohlavek, A.; Sikirić, M.D.; Kahru, A. Stability and toxicity of differently coated selenium nanoparticles under model environmental exposure settings. *Chemosphere* **2020**, 250, 126265, <https://doi.org/10.1016/j.chemosphere.2020.126265>.
 23. Amol, V.P.; Amol, A.S.; Vishwnath, R.P. Discrete SeNPs macromolecule binding manipulated by hydrophilic interaction. *Intern J Biol Macromol.* **2017**, 107, 1982–1987, <https://doi.org/10.1016/j.ijbiomac.2017.10.065>
 24. Association AD. Diagnosis and classification of diabetes mellitus. *Diabetes Care.* **2014**, 37, S81–S90, <https://doi.org/10.2337/dc14-S081>

25. Long, Y.C.; Cheng, Z.; Copp, K.D.; White, M.F. Insulin receptor substrates Irs1 and Irs2 coordinate skeletal muscle growth and metabolism via the Akt and AMPK pathways. *Mol Cell Biol.* **2011**, *31*, 430-441, <https://doi.org/10.1128/MCB.00983-10>.
26. Raza, H.; John, A. Streptozotocin-induced cytotoxicity, oxidative stress and mitochondrial dysfunction in human hepatoma HepG2 cells. *Int J Mol Sci.* **2012**, *13*, 5751-5767, <https://doi.org/10.3390/ijms13055751>.
27. Nova, E.; Redondo-Useros, N.; Martínez-García, R.M.; Gómez-Martínez, S.; Díaz- Prieto, L.E.; Marcos, A. potential of moringa oleifera to improve glucose control for the prevention of diabetes and related metabolic alterations: a systematic review of animal and human studies. *Nutrients.* **2020**, *12*, 2050, <https://doi.org/10.3390/nu12072050>.
28. Shirwaikar, A.; Rajendran, K.; Punitha, I.S.R. Anti-diabetic activity of alcoholic stem extract of *Coscinium fenestratum* in streptozotocin-nicotinamide induced type 2 diabetic rats. *J Ethnopharmacol.* **2005**, *97*, 369–374, <https://doi.org/10.1016/j.jep.2004.11.034>.
29. Benwahhoud, M.; Jouad, H.; Eddouks, M. Hypoglycemic effect of *Suaeda fruticosa* in streptozotocin-induced diabetic rats. *J Ethnopharmacol.* **2001**, *76*, 35–38, [https://doi.org/10.1016/s0378-8741\(01\)00207-0](https://doi.org/10.1016/s0378-8741(01)00207-0).
30. Mahdavi, A.; Bagherniya, M.; Mirenayat, M.S.; Atkin, S.L. Medicinal plants and phytochemicals regulating insulin resistance and glucose homeostasis in type 2 diabetic patients: a clinical review. *Adv Exp Med Biol.* **2021**, *1308*, 161-183, https://doi.org/10.1007/978-3-030-64872-5_13.
31. Maksoud, H.A.; Zaid, O.A.R.; Elharrif, M.G.; Omnia, M.A.; Alaa, E.A. Selenium clove droserifolia nanoparticles (Se-CNPs) and its ameliorative effects in experimentally induced diabetes mellitus. *Clin Nutr ESPEN.* **2020**, *40*, P383-391, <https://doi.org/10.1016/j.clnesp.2020.07.016>
32. Mahmoud, A.M.; Wilkinson, F.L.; McCarthy, E.M.; Moreno-Martinez, D.M.; Langford-Smith, A. Endothelial microparticles prevent lipid-induced endothelial damage via Akt/eNOS signaling and reduced oxidative stress. *FASEB J.* **2017**, *31*, 4636–4648, <https://doi.org/10.1096/fj.201601244RR> .
33. Ahangarpour, A.; Oroojan, A.A.; Khorsandi, L.; Kouchak, M.; Badavi, M. Hyperglycemia-induced oxidative stress in isolated proximal tubules of mouse: the in vitro effects of myricitrin and its solid lipid nanoparticle. *Arch Physiol Biochem.* **2021**, *127*, 422-428, <https://doi.org/10.1080/13813455.2019.1647250>.
34. Sasson, S. Nutrient overload, lipid peroxidation and pancreatic beta cell function. *Free Radic Biol. Med.* **2017**, *11*, 102–109, <https://doi.org/10.1016/j.freeradbiomed.2016.09.003>.
35. Adeyemi, D.O.; Ukwenya, V.O.; Obuotor, E.M.; Adewole, S.O. Antihepatotoxic activities of *Hibiscus sabdariffa* L. in animal model of streptozotocin diabetes-induced liver damage. *BMC Complement Altern Med.* **2014**, *14*, 277, <https://doi.org/10.1186/1472-6882-14-277>
36. Halse, R.; Bonavaud, S.M.; Armstrong, J.L.; McCormack, J.G.; Yeaman, S.J. Control of glycogen synthesis by glucose, glycogen, and insulin in cultured human muscle cells. *Diabetes* **2001**, *50*, 720–726, <https://doi.org/10.2337/diabetes.50.4.720>.
37. Zhang, Y.; Liu, D. Flavonol kaempferol improves chronic hyperglycemia-impaired pancreatic b-cell viability and insulin secretory function. *Eur J Pharmacol.* **2011**, *70*, 325–332, <https://doi.org/10.1016/j.ejphar.2011.08.011>.